RNA BIOLOGY
2017, VOL. 14, NO. 1, 113–123
http://dx.doi.org/10.1080/15476286.2016.1259782

Taylor & Francis
Taylor & Francis Group

RESEARCH PAPER

eIF4B stimulates eIF4A ATPase and unwinding activities by direct interaction through its 7-repeats region

Alexandra Zoi Andreou*, Ulf Harms*, and Dagmar Klostermeier

University of Muenster, Institute for Physical Chemistry, Muenster, Germany

ABSTRACT

Eukaryotic translation initiation starts with binding of the eIF4F complex to the 5′-m^{7}G cap of the mRNA. Recruitment of the 43S pre-initiation complex (PIC), formed by the 40S ribosomal subunit and other translation initiation factors, leads to formation of the 48S PIC that then scans the 5′-untranslated region (5′-UTR) toward the start codon. The eIF4F complex consists of eIF4E, the cap binding protein, eIF4A, a DEAD-box RNA helicase that is believed to unwind secondary structures in the 5′-UTR during scanning, and eIF4G, a scaffold protein that binds to both eIF4E and eIF4A. The ATPase and helicase activities of eIF4A are jointly stimulated by eIF4G and the translation initiation factor eIF4B. Yeast eIF4B mediates recruitment of the 43S PIC to the cap-bound eIF4F complex by interacting with the 40S subunit and possibly with eIF4A. However, a direct interaction between yeast eIF4A and eIF4B has not been demonstrated yet. Here we show that eIF4B binds to eIF4A in the presence of RNA and ADPNP, independent of the presence of eIF4G. A stretch of seven moderately conserved repeats, the r1-7 region, is responsible for complex formation, for modulation of the conformational energy landscape of eIF4A by eIF4B, and for stimulating the RNA-dependent ATPase- and ATP-dependent RNA unwinding activities of eIF4A. The isolated r1-7 region only slightly stimulates eIF4A conformational changes and activities, suggesting that communication of the repeats with other regions of eIF4B is required for full stimulation of eIF4A activity, for recruitment of the PIC to the mRNA and for translation initiation.

Abbreviations: ADPNP, 50-adenylyl-b,g-imidotriphosphate; DTT, dithiothreitol; eIF, eukaryotic translation initiation factor; FRET, fluorescence resonance energy transfer; UTR, untranslated region

ARTICLE HISTORY
Received 25 July 2016
Revised 5 November 2016
Accepted 8 November 2016

KEYWORDS
ATP hydrolysis; conformational change; DEAD-box helicase; eIF4A; regulation

Introduction

Initiation of translation in eukaryotes is mediated by a set of translation initiation factors (eIFs). The first step is the recognition of the 5′-m^{7}G cap of the mRNA by eIF4F, a heterotrimeric complex of the initiation factors eIF4A, eIF4G and eIF4E.[1] eIF4E is the cap-binding protein,[2,3] eIF4G is a scaffold protein that contacts both eIF4E and eIF4A,[1,4] and eIF4A is an RNA helicase of the DEAD-box family.[1,5] The 40S ribosomal subunit, bound to the initiation factor eIF2·GTP in complex with the initiator tRNA Met-tRNA$_i$ and to the initiation factors eIF1, eIF1A, eIF3 and eIF5, forms the 43S pre-initiation complex (PIC). The 43S PIC is recruited to the cap-bound eIF4F complex, and the resulting 48S PIC then scans the 5′-untranslated region (5′-UTR) of the mRNA toward the start codon. The helicase activity of eIF4A is thought to be required to disrupt secondary structures in the 5′-UTR and to displace bound proteins during ribosome scanning.[6,7] Once the start codon is reached, the 60S ribosomal subunit is recruited, and the elongation-competent 80S ribosome starts translation.

During unwinding of duplex regions, eIF4A alternates between an open conformation with a wide cleft between its two RecA domains, and a closed conformation in the presence of ATP and RNA, in which the two RecA domains interact with each other and with bound ATP and RNA.[8,9] Formation of the closed state is linked to duplex destabilization.[9,10] The translation initiation factors eIF4B and eIF4G jointly stimulate the weak intrinsic RNA-dependent ATPase and ATP-dependent RNA helicase activities of eIF4A,[11,12] by modulating the eIF4A conformational cycle.[9,13] eIF4G binds to eIF4A and stabilizes it in a half-open conformation[14] from which ADP and phosphate release[8] as well as RNA release[15] are accelerated. In the presence of eIF4G, eIF4A alternates between this half-open and the closed state,[13] and opening and closing are accelerated by eIF4G. eIF4B on its own does not affect the eIF4A conformational cycle, but stimulates closing when eIF4G is present.[9,13] Yeast eIF4B consists of an N-terminal domain (NTD), an RNA recognition motif (RRM), a region of seven repeats of moderate homology (r1-7), and a C-terminal domain[16,17] (CTD; Fig. 1). It has been shown previously that yeast eIF4B binds to 40S ribosomal subunits, and mediates recruitment of the PIC to the mRNA, possibly through interactions with eIF4A.[16] PIC recruitment depends on the presence of the r1-7 region of

CONTACT Dagmar Klostermeier dagmar.klostermeier@uni-muenster.de University of Muenster, Institute for Physical Chemistry, Corrensstrasse 30, D-48149 Muenster, Germany.
*These authors equally contributed to this work.

Supplemental data for this article can be accessed on the publisher's website.

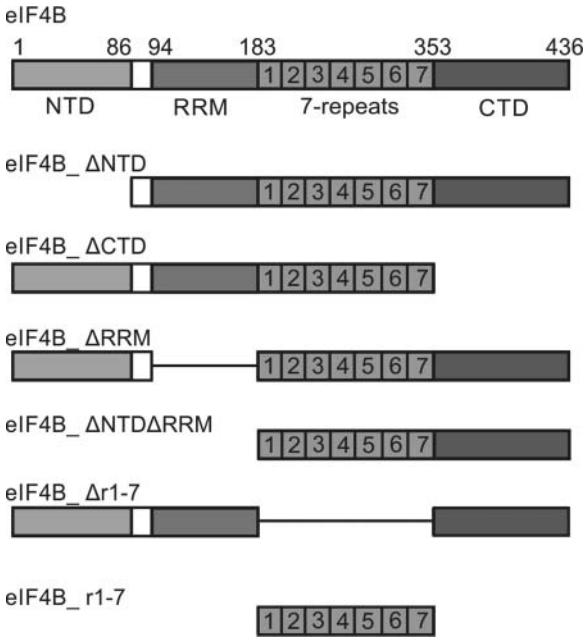

Figure 1. Yeast eIF4B constructs used in this study. eIF4B consists of an N-terminal domain (NTD), an RNA recognition motif (RRM), a 7-repeat region (r1-7), and a C-terminal domain (CTD). eIF4B deletion variants lacking one or multiple conserved regions were used in this study.

eIF4B, and to a lesser extent on the NTD.[16] Human eIF4A and eIF4B form a stable complex.[18,19] An equivalent interaction of yeast eIF4A and eIF4B was deduced from genetic studies,[20,21] the stimulation of the eIF4A helicase activity by eIF4B,[9] and the observation that eIF4B promotes the interaction of eIF4A with the PIC,[16] but the formation of a yeast eIF4A/eIF4B complex has not been observed experimentally. Here we show that yeast eIF4B interacts directly with eIF4A in the presence of RNA and the non-hydrolyzable analog ADPNP, independent of eIF4G. The r1-7 region of eIF4B is required for the interaction between eIF4A and eIF4B, and for the modulation of the eIF4A conformational cycle and the stimulation of the eIF4A activities by eIF4B.

Results

Complex formation of yeast eIF4B with eIF4A in the presence of RNA

The molecular mechanism by which eIF4B modulates the activity of the RNA helicase eIF4A has long been a subject of debate. Stable eIF4A/eIF4B complexes have been identified in pull-down experiments for the mammalian counterparts only.[18,19] A direct interaction of yeast eIF4A and eIF4B is supported by the observed stimulation of the eIF4A helicase activity by eIF4B[9] and the promotion of the eIF4A-PIC interaction by eIF4B,[16] and by genetic studies,[20] but has not been shown experimentally. In conventional binding experiments (such as size-exclusion chromatography or pull-down experiments) reactants are mixed at concentrations that favor complex formation, but multiple washing steps and the concomitant dilution may allow dissociation of the binding partners. To identify a possible yeast eIF4A/eIF4B complex without these dilution effects, we used a supernatant depletion assay previously described by Pollard[22] (Fig. 2A). N-terminally biotinylated eIF4A (eIF4A-bio)[13] immobilized on streptavidin beads was added in increasing amounts to samples containing constant concentrations of eIF4B or Alexa488-labeled eIF4B (eIF4B_248C/274C), RNA (32mer) and the non-hydrolyzable

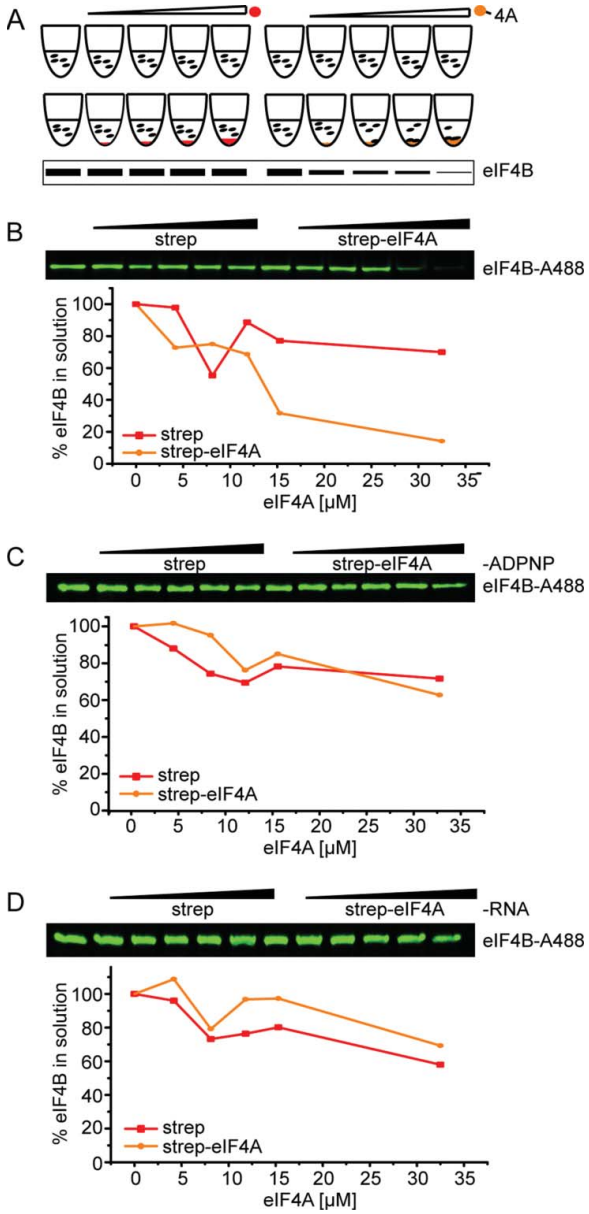

Figure 2. eIF4B binds to eIF4A in the presence of ADPNP and RNA. (A) Schematic overview of the supernatant depletion assay after Pollard *et al.*[22] to probe binding of eIF4B to eIF4A. Increasing amounts of streptavidin beads with immobilized biotinylated eIF4A (eIF4A-bio, orange sphere) or without (negative control, red sphere) were incubated with a constant concentration of eIF4B or Alexa-488 labeled eIF4B (eIF4B-A488). The supernatant is analyzed by SDS-PAGE. A decrease of protein in the supernatant reflects binding to eIF4A-bio. (B) Supernatant depletion assay to follow binding of 0.25 μM eIF4B-A488 (eIF4B_248C/274C) to eIF4A-bio in the presence of 5 μM RNA (32mer) and 10 mM ADPNP (Coomassie Blue staining). eIF4A-bio concentrations are 0, 4, 8, 12, 15 and 33 μM. eIF4B in the supernatant was quantified from the fluorescence intensity. Red: depletion upon addition of streptavidin beads (negative control), yellow: depletion upon addition of eIF4A-conjugated streptavidin beads. Data shown are a representative example of two independent experiments (see Fig. 3C). (C), (D) Supernatant depletion assay with eIF4B in the absence of ADPNP or RNA.

ATP analog 5′adenylyl-ß,γ-imidotriphosphate 5′adenylyl-ß,γ-imidotriphosphate (ADPNP). The intracellular concentrations of eIF4A and eIF4B in yeast are in the range of 50–60 μM and around 15 μM, respectively.[23] The concentrations of translation initiation factors used in the assay (0–33 μM eIF4A, 0.25–0.5 μM eIF4B) are therefore in a physiologically relevant range. A decrease of eIF4B in the supernatant with increasing concentrations of eIF4A was observed, in agreement with binding of eIF4B to eIF4A in the presence of RNA and ADPNP. In control reactions with streptavidin beads lacking eIF4A, the depletion of eIF4B in the supernatant was negligible (Fig. 2B, Fig. S1). Binding of eIF4B to eIF4A was not observed when either ADPNP or RNA was omitted (Fig. 2C,D), demonstrating that a stable interaction between eIF4A and eIF4B requires the presence of RNA and nucleotide.

Formation of a stable complex of mammalian eIF4A and eIF4B requires the presence of eIF4G,[19] yet we observe the interaction between yeast eIF4A and eIF4B in the absence of eIF4G. We next probed if yeast translation initiation factor eIF4G had any effect on the interaction of eIF4B with eIF4A, using eIF4G_572-952 (eIF4G) which comprises the middle domain responsible for eIF4A binding and the C-terminal R/S-rich tail that contributes to the stimulation of eIF4A activities.[9] eIF4G alone formed a stable complex with immobilized eIF4A in the absence of RNA and ADPNP, as evidenced by a decrease of eIF4G in the supernatant with increasing eIF4A concentrations (Fig. 3A). In experiments with eIF4B and eIF4G (and RNA and ADPNP), both eIF4B and eIF4G were depleted from the supernatant, in agreement with binding of both factors to eIF4A (Fig. 3B,C, Fig. S2B,C). However, no effect of eIF4G on eIF4B binding to eIF4A or of eIF4B on binding of eIF4G to eIF4A was observed (Fig. 3C, Fig. S2C). Thus, yeast eIF4B binding to eIF4A in the presence of RNA and ADPNP is independent of eIF4G. The concentrations of eIF4G in these experiments are in the range of the intracellular concentration of eIF4G in yeast,[23] and hence physiologically relevant.

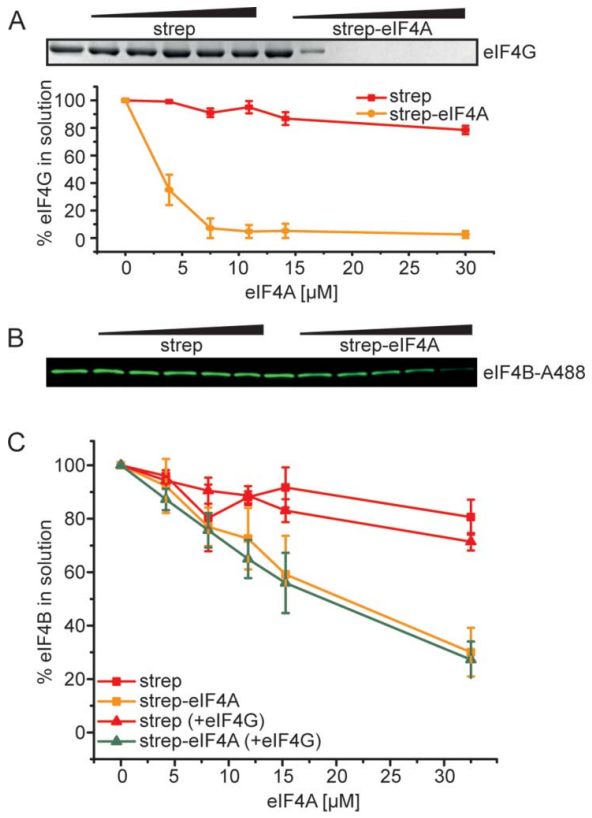

Figure 3. eIF4B and eIF4G bind independently to eIF4A. (A) Supernatant depletion assay with 0, 4, 8, 12, 15 and 33 μM eIF4A-bio and 2 μM eIF4G in the absence of RNA and ADPNP (Coomassie Blue staining). eIF4G in the supernatant was quantified by densitometry. Red: depletion upon addition of streptavidin beads (negative control), yellow: depletion upon addition of eIF4A-conjugated streptavidin beads. The quantification shows data from two independent experiments in the absence and presence of RNA and ADPNP; error bars reflect the standard errors of the mean. (B) Supernatant depletion assay to follow binding of 0.25 μM eIF4B-A488 to eIF4A-bio in the presence of 10 mM ADPNP, 5 μM RNA (32mer) and 15 μM eIF4G (fluorescence detection). (C) Quantification of eIF4B in the supernatant from the fluorescence intensity. eIF4B binds with comparable affinity to streptavidin-bound eIF4A-bio in the absence (orange) or presence (green) of 15 μM eIF4G. Control experiments with unconjugated streptavidin beads are depicted in red. Mean values from two independent experiments (see Fig. S2) with standard errors.

Identifying domains of eIF4B implicated in eIF4A activation (I): The 7-repeats (r1-7) region is essential for stimulating eIF4A ATPase activity

We next dissected the role of individual eIF4B domains for the activation of eIF4A. To this end, eIF4B deletion variants lacking one or multiple domains[16] were analyzed for their stimulatory effect on eIF4A ATPase and RNA unwinding activities (Fig. 4, Table 1). We have recently demonstrated that yeast eIF4B alone does not stimulate the eIF4A ATPase activity.[9] In the presence of eIF4G, eIF4B stimulates eIF4A ATPase activity by decreasing the apparent K_M of eIF4A for RNA ($K_{M,app,RNA}$) without affecting k_{cat}.[9] To identify the eIF4B domain responsible for the stimulation of eIF4A ATPase activity in conjunction with eIF4G, we determined rates of ATP hydrolysis by eIF4A in the presence of eIF4G and different eIF4B deletion variants as a function of RNA concentration (Fig. 4A). As an RNA substrate, we used poly(U)-RNA, a single-stranded RNA frequently used as a non-specific model substrate for DEAD-box helicases. The $K_{M,app,RNA}$ of 104 ± 15 μM for the eIF4A/eIF4G complex was decreased 6-fold to 18 ± 1 μM in the presence of eIF4B (Fig. 4B), in agreement with previous studies.[9] The turnover number was independent of eIF4B, with $k_{cat} = 81 \pm 4\times10^{-3}$ s^{-1} (− eIF4B) and k_{cat}

Table 1. Stimulation of eIF4A ATPase and unwinding activities by eIF4B and eIF4B deletion variants. eIF4A ATPase activity with k_{cat} and $K_{M,app,RNA}$ and rate constants for RNA unwinding by eIF4A in the presence of the different eIF4B variants, k_{unwind}, with the standard deviations determined from at least 3 different experiments. ATPase experiments in presence of eIF4B_r1–7 were performed in duplicates and values are given with the standard error (SE).

Proteins	k_{cat} [10^{-3} s^{-1}]	$K_{M,app,RNA}$ [μM]	k_{unwind} [10^{-3} s^{-1}]
eIF4A	5 ± 1	15 ± 6	0.08 ± 0.06
eIF4A+eIF4G	81 ± 4	104 ± 15	0.45 ± 0.13
eIF4A+eIF4G+eIF4B[1]	86 ± 3	18 ± 1	1.60 ± 0.25
eIF4A+eIF4G+eIF4B_ΔNTD	84 ± 5	31 ± 3	1.52 ± 0.07
eIF4A+eIF4G+eIF4B_ΔCTD	90 ± 3	18 ± 2	1.35 ± 0.29
eIF4A+eIF4G+eIF4B_ΔRRM	85 ± 3	31 ± 6	1.07 ± 0.28
eIF4A+eIF4G+eIF4B_ΔNTDΔRRM	77 ± 1	35 ± 5	1.09 ± 0.21
eIF4A+eIF4G+eIF4B_Δr1–7	85 ± 7	127 ± 17	0.48 ± 0.09
eIF4A+eIF4G+eIF4B_r1–7	74 ± 4 (SE)[2]	66 ± 15 (SE)[2]	0.63 ± 0.21

[1]eIF4B on its own has no effect on k_{cat} and $K_{M,app,RNA}$ values, but causes a 5-fold increase in k_{unwind} (see [9]).
[2]SE = standard error from two independent experiments.

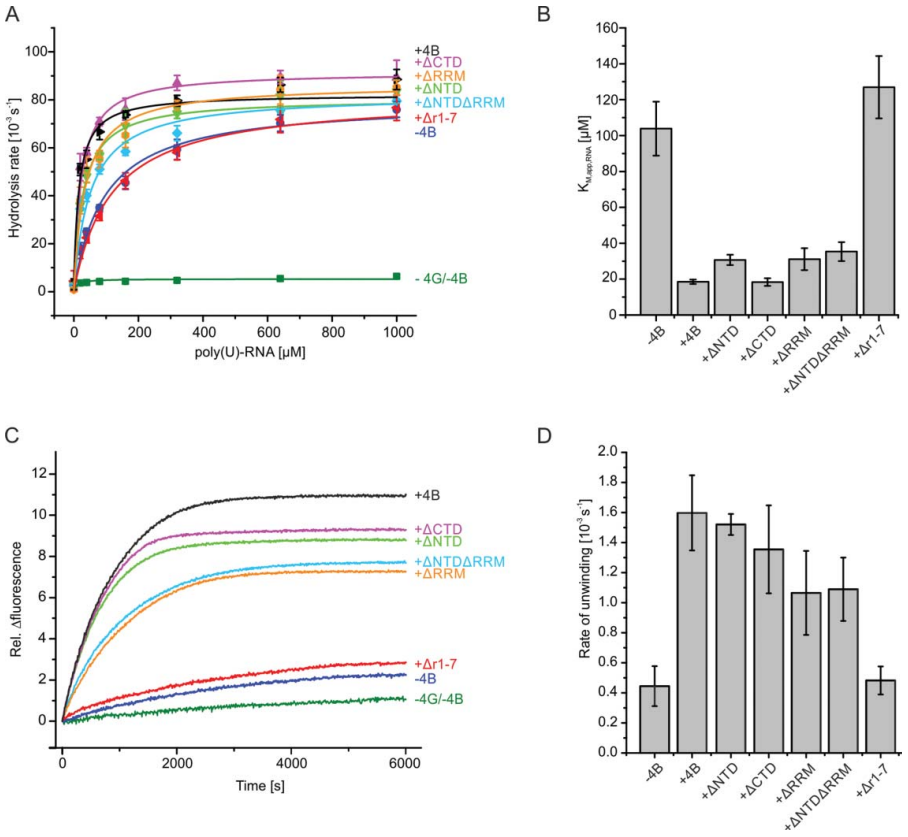

Figure 4. The r1–7 region is crucial for stimulating eIF4A unwinding and ATPase activities. (A) Effects of eIF4B variants on ATP hydrolysis by eIF4A. eIF4A in the absence of other factors (green squares), in the presence of eIF4G (blue circles) or in the presence of eIF4G and eIF4B (black triangles), eIF4B_ΔNTD (light green triangles), eIF4B_ΔCTD (purple triangles), eIF4B_ΔNTDΔRRM (cyan diamonds), eIF4B_ΔRRM (orange hexagons) or eIF4B_Δr1–7 (red triangles). Each point is the mean of three independent experiments, error bars reflect the standard deviation. Data are described with the Michaelis-Menten equation. See text and Table 1 for k_{cat} values and apparent Michaelis-Menten constants ($K_{M,app,RNA}$). (B) $K_{M,app,RNA}$ values for eIF4A in the presence of eIF4G and eIF4B variants from data shown in A). Error bars represent the standard deviation from at least three independent experiments. (C) Representative time courses of RNA unwinding by eIF4A and the effect of eIF4G, eIF4B and eIF4B variants on unwinding. Unwinding is initiated by adding saturating concentrations of ATP, and is followed by a decrease in FRET (i.e. decrease in Cy5 fluorescence, plotted here as an increase to facilitate comparison with A). eIF4A (green), eIF4A and eIF4G (blue), eIF4A, eIF4G and eIF4B (black), eIF4A, eIF4G and eIF4B_ΔNTD (light green), eIF4A, eIF4G and eIF4B_ΔCTD (purple), eIF4A, eIF4G and eIF4B_ΔRRM (orange), eIF4A, eIF4G and eIF4B_ΔNTDΔRRM (cyan), or eIF4A, eIF4G and eIF4B_Δr1–7 (red). Data were described by a single exponential function to determine unwinding rate constant. (D) Unwinding rate constants for eIF4A in the presence of eIF4G and the different eIF4B variants. Values are means from at least three independent measurements; error bars reflect the standard deviation. The 9 bp duplex of the unwinding substrate has a calculated thermodynamic stability of $\triangle G = -84$ kJ mol^{-1} at 25°C (mfold version 2.3). [37]

$= 86 \pm 3\times10^{-3}$ s^{-1} (+ eIF4B), respectively. eIF4B variants lacking the NTD (eIF4B_ΔNTD; $K_{M,app,RNA} = 31 \pm 3$ μM) or the CTD (eIF4B_ΔCTD; $K_{M,app,RNA}$ 18 ± 2 μM) led to a similar reduction in $K_{M,app,RNA}$ as full-length eIF4B. The eIF4B variant lacking the RRM (eIF4B_ΔRRM) decreased the $K_{M,app,RNA}$ to 31 ± 6 μM, and the variant lacking both RRM and NTD (eIF4B_ΔNTDΔRRM) caused a reduction to $K_{M,app,RNA} = 35 \pm 5$ μM. Strikingly, the presence of the eIF4B_Δr1-7 variant lacking the 7-repeats region did not cause a decrease in $K_{M,app,RNA}$ ($K_{M,app,RNA} = 127 \pm 17$ μM). These results identify the r1-7 region of eIF4B as a key player in the stimulation of the eIF4A ATPase activity by eIF4B *in vitro*, while the NTD, CTD and the RRM play minor roles in ATPase stimulation.

Identifying domains of eIF4B implicated in eIF4A activation (II): Efficient duplex separation by eIF4A requires the r1-7 region

Unwinding of a variety of RNA substrates by eIF4A is stimulated by eIF4G, eIF4H and eIF4B.[6,9,11,18,24-26] We next determined the unwinding activity of eIF4A and its response to eIF4B variants using a donor-acceptor-labeled 32/9mer RNA as a substrate (Fig. 4 C,D, Table 1). This RNA, consisting of a 9 base-pair duplex region adjacent to hairpin 92 of 23S rRNA, has previously been used in unwinding[9,27,28] and single-molecule FRET experiments.,[9,13] RNA unwinding was followed by a decrease in acceptor (Cy5) fluorescence. In agreement with previous studies eIF4A showed very low intrinsic helicase activity[6,9,11,18,24-26] and unwound the 32/9mer with a rate constant of $k_{unwind} = 0.08$ (±0.06) × 10^{-3} s^{-1} (Fig. 4 C,D). The rate constant of unwinding increased 5-fold in the presence of eIF4G to $k_{unwind} = 0.45$ (±0.13) × 10^{-3} s^{-1}, and increased an additional 4-fold to $k_{unwind} = 1.60$ (±0.25) × 10^{-3} s^{-1} upon addition of eIF4B. This rate constant is comparable to previously reported rate constants of $k_{unwind} = 1.7 \times 10^{-3}$ s^{-1}, [29] or $k_{unwind} = 2.4 \times 10^{-3}$ s^{-1}.[9] All unwinding reactions were performed in presence of a 9mer RNA trap to ensure single turnover conditions. Similar unwinding rates were observed when a 9mer DNA was used as a trap (Fig. S3). We next investigated RNA unwinding by the eIF4A/eIF4G complex in the presence of the eIF4B deletion variants (Fig. 4 C,D). eIF4B_ΔNTD and eIF4B_ΔCTD stimulated eIF4A unwinding activity to a similar

extent as full-length eIF4B, with $k_{unwind} = 1.52\ (\pm 0.07) \times 10^{-3}\ s^{-1}$ (eIF4B_ΔNTD) and $k_{unwind} = 1.35\ (\pm 0.29) \times 10^{-3}\ s^{-1}$ (eIF4B_ΔCTD), respectively. These domains are therefore dispensable for the stimulation of eIF4A unwinding activity. eIF4B_ΔRRM or eIF4B_ΔNTDΔRRM were only slightly less efficient in stimulating eIF4A unwinding activity, with $k_{unwind} = 1.07\ (\pm 0.28) \times 10^{-3}\ s^{-1}$ (eIF4B_ΔRRM) and $k_{unwind} = 1.09\ (\pm 0.21) \times 10^{-3}\ s^{-1}$ (eIF4B_ΔNTDΔRRM). Thus, the RNA binding function of the RRM does not seem to be essential for duplex separation by eIF4A. The CTD, NTD, and the RRM are not required for the stimulation of the eIF4A helicase activity by eIF4B. The deletion variant lacking the r1–7 region, eIF4B_Δr1-7, in contrast, failed to stimulate unwinding of the 32/9mer by eIF4A, and the rate constant ($k_{unwind} = 0.48\ (\pm 0.09) \times 10^{-3}\ s^{-1}$) was the same as in the absence of eIF4B ($k_{unwind} = 0.45\ (\pm 0.13) \times 10^{-3}\ s^{-1}$). Again, using a DNA trap instead of RNA gave similar results (Fig. S3). Thus, the r1–7 region plays a key role in the mechanism of activation of the eIF4A helicase by eIF4B.

Identifying eIF4B domains implicated in eIF4A activation (III): Closing the cleft between the eIF4A domains depends on the r1-7 region of eIF4B

eIF4A on its own, in the absence of other translation initiation factors, very rarely undergoes conformational changes to the closed conformation in the presence of RNA and ATP,[9,13] in agreement with its low intrinsic ATPase and helicase activities. When eIF4G is present, eIF4A dynamically switches between a half-open conformation, stabilized by eIF4G,[8,14] and the closed state.[9,13] We have previously shown that the addition of eIF4B to an eIF4A/eIF4G complex further shifts the conformational equilibrium of eIF4A toward the closed state by selectively increasing the closing rate of eIF4A.[9,13] To identify the eIF4B domain which is responsible for modulation of the eIF4A conformational landscape, we performed single molecule FRET experiments with donor/acceptor-labeled eIF4A in the presence of the eIF4B variants, eIF4G, poly(U)-RNA and ATP (Fig. 5; Fig. S4). The effects of eIF4B variants on the population of the closed state in equilibrium were determined from the relative population of the high-FRET state reflecting the closed eIF4A species before and after addition of eIF4B. In agreement with previous observations, eIF4A adopted low- and high-FRET states in the presence of eIF4G, ATP and RNA, corresponding to the half-open and closed conformations; respectively[9] (Fig. 5A). The increase in the population of the closed eIF4A conformation upon addition of eIF4B was 14% (Fig. 5B), again consistent with previous findings.[9] A similar increase (12- 13%) was observed in the presence of eIF4B_ΔCTD, ΔNTD, ΔRRM and ΔNTDΔRRM (Fig. 5D-G). In contrast, the population of the closed state of eIF4A remained unaffected upon addition of eIF4B_Δr1-7 (Fig. 5C). The r1–7 region is thus crucial for promoting formation of the closed state of eIF4A, and hence for stimulation of ATPase and RNA unwinding activities.

The r1-7 region of eIF4B is necessary for binding to eIF4A

To understand why the r1-7 region is so important for the stimulation of eIF4A activities, we tested binding of the eIF4B deletion variants to eIF4A in the supernatant depletion assay (Fig. 6). eIF4B_ΔCTD and eIF4B_ΔNTDΔRRM showed binding to eIF4A in similar concentration ranges as full-length eIF4B (Fig. 6A,B), demonstrating that the NTD, RRM and CTD are dispensable for eIF4A/eIF4B complex formation. Notably, eIF4B_Δr1-7 did not show any interaction with eIF4A and remained in the supernatant at a constant concentration both in the absence and presence of eIF4G (Fig. 6C, Fig. S5). Thus, the r1-7 region is central for eIF4A activation by eIF4B because it mediates binding of eIF4B to eIF4A.

The r1-7 region on its own does not fully stimulate eIF4A activities

We next tested whether the isolated r1–7 region may be sufficient to mediate stimulation of eIF4A activities (Fig. 7, Table 1). Addition of eIF4B_r1–7 to eIF4A in the presence of eIF4G, RNA and ATP had only a moderate effect on $K_{M,app,RNA}$, which decreased from $K_{M,app,RNA} = 103 \pm 15\ \mu M$ in its absence to $K_{M,app,RNA} = 66 \pm 15\ \mu M$ in its presence (Fig. 7A, Table 1). Likewise, the rate of RNA unwinding by eIF4A increased only slightly (from $k_{unwind} = 4.5 \times 10^{-4}\ s^{-1}$ to $k_{unwind} = 6.3 \times 10^{-4}\ s^{-1}$ in the presence of eIF4B_r1–7 (Fig. 7B, Table 1). Single molecule FRET experiments revealed a moderate increase of the eIF4A population in the closed state by 9% upon addition of eIF4B_r1-7 (Fig. 7C) (compared to 13% for full-length eIF4B; Fig. 5B,H). Altogether, the isolated r1-7 region thus appeared to be able to at least partially recapitulate the stimulatory effect of eIF4B on eIF4A. We therefore examined whether eIF4B_r1–7 on its own still binds to eIF4A in the presence of eIF4G, RNA and ADPNP in supernatant depletion assays (Fig. 7D). The concentration of eIF4B_r1–7 in the supernatant indeed decreased with increasing concentrations of eIF4A, although to a lesser extent than with full-length eIF4B. Altogether, the r1-7 region thus plays a central role in mediating the interaction of eIF4B with eIF4A, in promoting the conformational change of eIF4A to the closed state, and in stimulating the ATPase and RNA unwinding activities of eIF4A. However, the isolated r1-7 region is not able to fully emulate the stimulatory effects of eIF4B.

Discussion

In this study we analyzed the physical and functional interaction between yeast translation initiation factors eIF4A and eIF4B. We could show that eIF4A and eIF4B physically interact in an RNA- and nucleotide-dependent manner and that the interaction is not eIF4G-mediated. Using eIF4B deletion variants we determined that the r1-7 region is crucial for the association of eIF4B with eIF4A, and a key element for the stimulation of eIF4A ATPase and unwinding activities and for promotion of the eIF4A conformational change to the closed state.

A physical interaction of eIF4A and eIF4B is conserved from yeast to humans and plants

An interaction of yeast eIF4A and eIF4B has previously been inferred from genetics studies,[20] and from the stimulation of the eIF4A helicase activity[9] as well as its functional interaction with eIF4A in PIC recruitment,[16] but to date had not been observed directly. Using a supernatant depletion assay we could

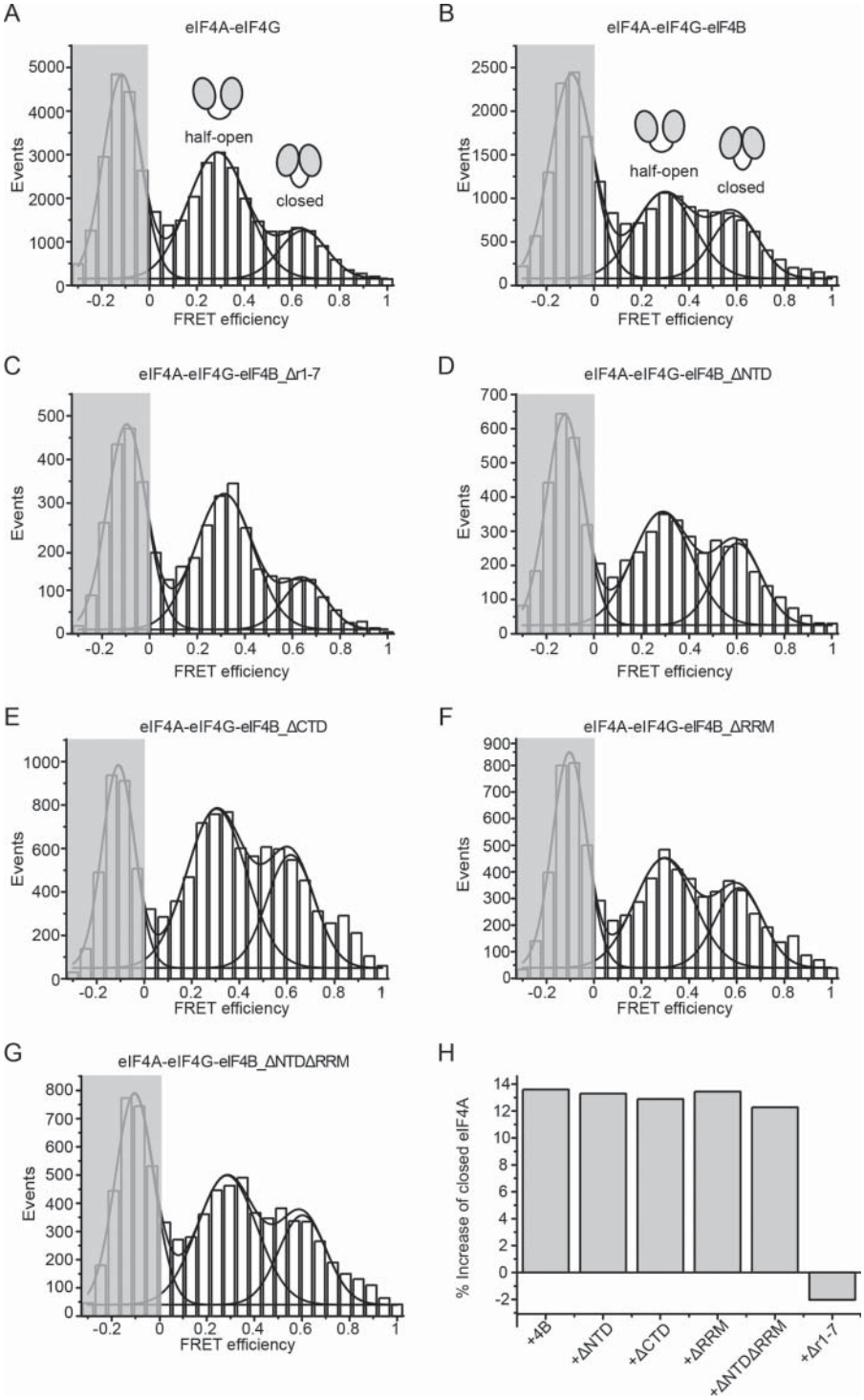

Figure 5. eIF4B_Δr1–7 fails to stimulate the eIF4A conformational change to the closed state. (A) single molecule FRET histogram for donor- and acceptor-labeled eIF4A in the presence of eIF4G, poly(U) RNA and ATP, accumulated from three independent experiments (see Fig. S4). The histograms were described by a sum of Gaussian distributions to extract fractional populations. The peak in the shaded area corresponds to eIF4A molecules that carry only donor fluorophores. The low- and high-FRET species with FRET efficiencies of 0.29 and 0.65 reflect the half-open and closed conformations of eIF4A, respectively.[8,9,13] (B) Addition of eIF4B to eIF4A/eIF4G increases the population of the closed state by 13% compared to (A). (C) Addition of eIF4B_Δr1–7 to eIF4A/eIF4G does not change the fractional populations of eIF4A of the half-open and closed states. (D) to (G) smFRET histograms for eIF4A in the presence of eIF4G and eIF4B_ΔNTD, eIF4B_ΔCTD, eIF4B_ΔRRM or eIF4B_ΔNTDΔRRM. Addition of these mutants increase the closed eIF4A conformation between 12 to 13% which is comparable to wild-type eIF4B. (H) Relative change in the closed population of eIF4A upon addition of the eIF4B variants to eIF4A/eIF4G.

detect a direct interaction between yeast eIF4A and eIF4B in presence of RNA and nucleotide, in agreement with the ability of eIF4B to stimulate eIF4A unwinding activity in absence of other translation initiation factors.[9] Although the supernatant depletion assays are not quantitative, they provide an estimate for the K_d value of the eIF4A/eIF4B complex in the micromolar range, which explains why the interaction has not been detected by size-exclusion chromatography or pull down experiments

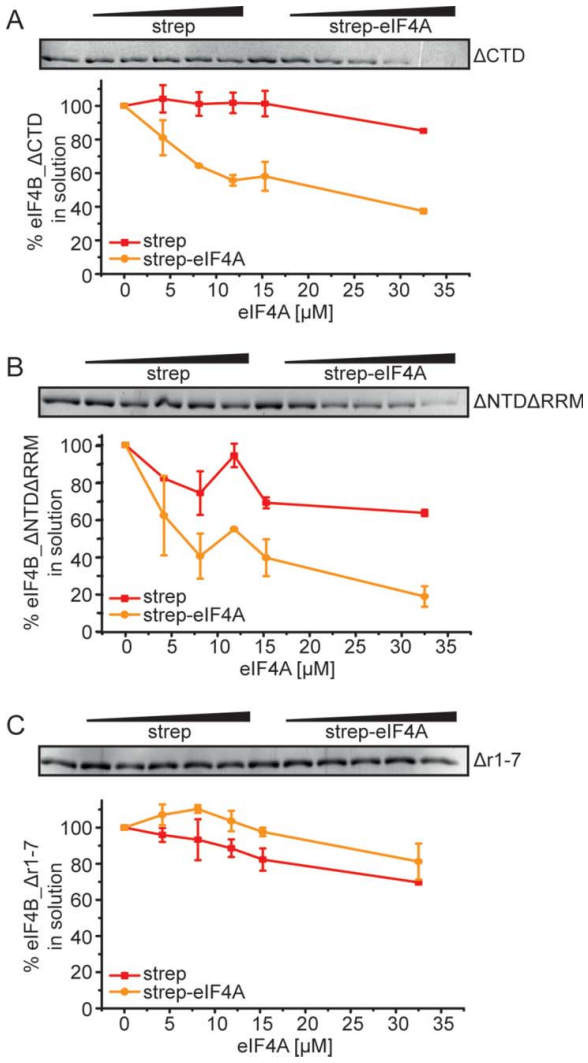

Figure 6. The r1–7 region is required for eIF4B binding to eIF4A. Supernatant depletion assay with eIF4A-bio and 0.5 μM of either eIF4B_ΔCTD (A), eIF4B_ΔNTDΔRRM (B) or eIF4B_Δr1–7 (C) in the presence of 5 μM 32mer RNA and 10 mM ADPNP (Coomassie Blue staining). eIF4B in the supernatant was quantified by densitometry. Red: depletion upon addition of streptavidin beads (negative control), yellow: depletion upon addition of eIF4A-conjugated streptavidin beads. The quantification shows the mean values from 2 independent experiments with standard errors.

where dilution effects lead to dissociation of low-affinity complexes. The yeast eIF4A/eIF4B complex thus appears to be less stable than the corresponding complex of human eIF4A and eIF4B.[11,18] This difference in complex stability may explain why yeast eIF4B achieves only a moderate stimulation of eIF4A activities on its own, with no effect on ATPase rates and a 5-fold stimulation of RNA unwinding (Table 1),[9] compared to a stimulation of the ATPase activity of human eIF4A by eIF4B by 3-fold and a 20-fold increase in RNA unwinding rates.[29]

eIF4B is the least conserved of the eukaryotic translation initiation factors.[30] Despite the structural differences of yeast and mammalian eIF4B, yeast eIF4A is activated by mammalian eIF4B[31] and mammalian eIF4B can substitute for yeast eIF4B in cell-free translation,[32] suggesting that yeast and mammalian eIF4B have conserved functions. Our findings that yeast eIF4A interacts with eIF4B in a nucleotide- and RNA-dependent manner, just like the mammalian counterparts,[18,19] provide further support for a functional similarity between mammalian and yeast eIF4B. Wheat eIF4A and eIF4B associate in the absence of nucleotide or RNA,[33] in agreement with a conserved interaction between these proteins from yeast to mammals and plants, but different requirements for complex formation.

Why is the eIF4A-eIF4B interaction RNA- and nucleotide-dependent?

The RNA- and nucleotide-dependent association of yeast eIF4A and eIF4B could in principle be rationalized by three different scenarios, (1), binding of eIF4B to the closed conformation of eIF4A (2), an interaction of RNA-bound, but not of free eIF4B with eIF4A, or (3) an RNA-mediated interaction with eIF4A and eIF4B bound to the same RNA. An RNA-mediated interaction would be consistent with the larger footprint of eIF4A on RNA when eIF4B is present.[18] Priming of eIF4B for interaction with eIF4A by RNA binding has been suggested previously.[19] The 32mer RNA is indeed bound by eIF4B ($K_d = 0.94$ (± 0.18 μM,[9]). Under the conditions of the supernatant depletion assays, the saturation of eIF4B with RNA is ~84%. The eIF4B_ΔNTDΔRRM variant has severely reduced RNA affinity.[16] Its affinity for the 32mer complex is decreased 14-fold compared to full-length eIF4B, with K_d = 13.4 (± 0.6 μM (Fig. 8), corresponding to a saturation with RNA of only ~27% in the supernatant depletion assays. Despite this three-fold lower saturation with RNA, eIF4B_ΔNTDΔRRM is depleted from the supernatant to the same extent as eIF4B, indicating that RNA binding to eIF4B is not a major determinant for the interaction with eIF4A. Thus, the wild-type-like interaction of eIF4B_ΔNTDΔRRM with eIF4A argues against a requirement for RNA-bound eIF4B, and against an RNA-mediated interaction.

eIF4A does not bind the 32mer in the absence of nucleotide, but in the presence of 10 mM ADPNP a complex with K_d = 10.3 $\pm$ 1.3 μM is formed (Fig. 8). The saturation of eIF4A with 32mer RNA in the supernatant depletion assays is ~11% at the highest concentration (33 μM). These ~11% of RNA-bound eIF4A, and thus of eIF4A in the closed state, correspond to an absolute concentration of ~0.3 μM (compared to 0.5 μM eIF4B), which would be sufficient to account for the observed depletion of eIF4B from the supernatant. Hence, eIF4B most likely binds to the closed, RNA- and ADPNP-bound state of eIF4A.

Yeast eIF4B and eIF4G bind independently to eIF4A

A number of studies have focused on the functional interplay between initiation factors eIF4B and eIF4G and showed that these factors stimulate eIF4A activity synergistically.[9,13,19,29,34] While complex formation of human eIF4A and eIF4B requires catalytic amounts of eIF4G,[19] the interaction of yeast eIF4B with eIF4A already occurs in the absence of eIF4G, and is not promoted by the presence of catalytic or stoichiometric concentrations of eIF4G. Our supernatant depletion assays are consistent with binding of both eIF4B and eIF4G to yeast eIF4A, and thus with formation of a ternary complex. Formation of a ternary complex would rationalize why eIF4B can promote the association of eIF4A with eIF4G variants that show reduced

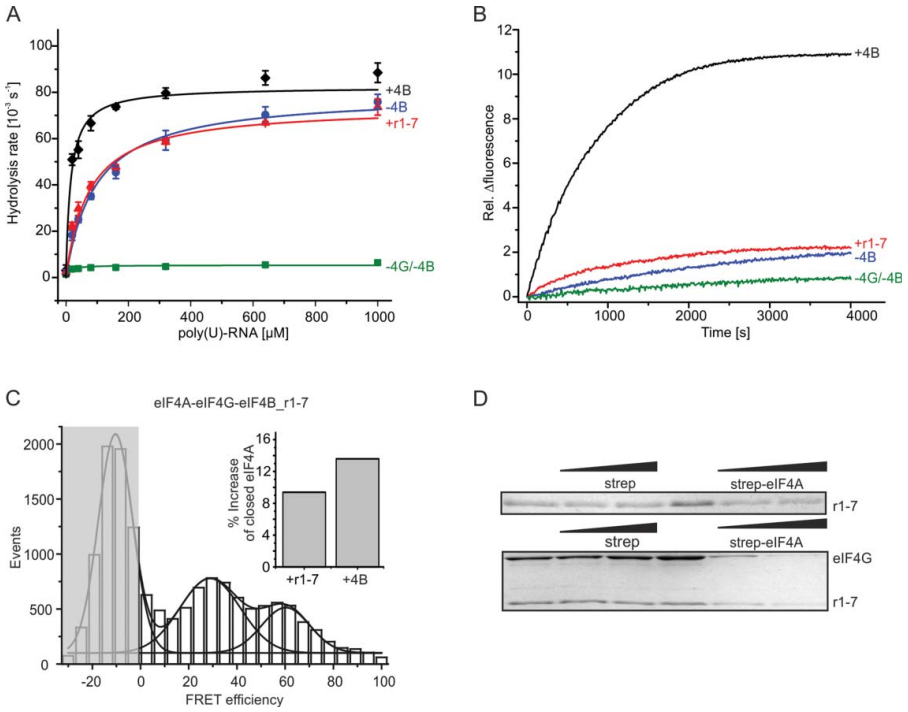

Figure 7. The eIF4B_r1-7 region in isolation only slightly stimulates eIF4A activities. (A) Effect of eIF4B_r1-7 on ATP hydrolysis by eIF4A; eIF4A only (green squares), eIF4A and eIF4G (blue circles), eIF4A, eIF4G and eIF4B (black diamonds) or eIF4A, eIF4G and eIF4B_r1–7 (red triangles). Data were described with the Michaelis Menten equation. The $K_{M,app,RNA}$ values are 104 ± 15 μM (eIF4A, eIF4G), 18 ± 1 μM (eIF4A, eIF4G, eIF4B) or 66 ± 15 μM (eIF4A, eIF4G, eIF4B_r1–7). The $K_{M,app,RNA}$ for eIF4B_r1-7 is the mean of 2 independent experiments ± standard error. (B) Representative unwinding time courses for eIF4A (green), eIF4A and eIF4G (blue), eIF4A, eIF4G and eIF4B (black) or eIF4A, eIF4G and eIF4B_r1–7 (red). The unwinding rate of eIF4A in the presence of eIF4B and eIF4B_r1–7 is slightly increased to 0.63 ± 0.21 10^{-3} s^{-1}. (C) smFRET histogram for donor- and acceptor-labeled eIF4A in the presence of eIF4G, eIF4B_r1–7, poly(U) RNA and ATP. The inset shows the relative change in the closed population of eIF4A upon the addition of eIF4B (13%) or eIF4B_r1–7 (9%) to eIF4A/eIF4G. (D) Supernatant depletion assay with 0, 15 and 33 μM eIF4A-bio and 0.5 μM eIF4B_r1–7 in the absence (top) and presence of 2 μM eIF4G (bottom). The concentration of eIF4B_r1–7 in the supernatant is reduced in both cases, suggesting binding of the r1–7 region to eIF4A independent of eIF4G.

eIF4A affinities,[21] and is in agreement with the synergistic activation of eIF4A by eIF4B and eIF4G.[9,13]

Stimulation of eIF4A ATPase and helicase activities requires the r1-7 region

Yeast eIF4B and eIF4G jointly activate eIF4A ATP hydrolysis and couple it to RNA unwinding activity[9,29] by modulating eIF4A conformational cycling between a half-open and a closed state.[9,13] We have shown here that eIF4B variants lacking either the NTD, CTD or the RRM bind to eIF4A, stimulate eIF4A ATPase and RNA unwinding activities and promote a conformational change of eIF4A toward the closed state, similar to full-length eIF4B. In contrast, eIF4B lacking the r1–7 region does not form a complex with eIF4A, and hence fails to stimulate eIF4A activities. Binding cannot be rescued by eIF4G. The same eIF4B construct lacking the r1–7 region exhibits defects in PIC recruitment to the mRNA *in vitro*[16] and leads to a slow growth phenotype *in vivo*,[16,35] According to secondary structure predictions, eIF4B contains little secondary structure. Circular dichroism spectra are consistent with the prediction, and similar for eIF4B and eIF4B_Δr1-7 (Fig. S6), rendering it unlikely that the loss of function of eIF4B lacking the r1-7 region is due to misfolding. We can therefore attribute the failure of eIF4B_Δr1-7 to stimulate eIF4A activities and to promote PIC recruitment to a lack of complex formation between eIF4B and eIF4A.

Interestingly, both eIF4B_ΔNTDΔRRM and eIF4B_Δr1–7 have severely reduced RNA affinities,[16] yet they show very different interactions with eIF4A (wild-type like versus no binding), which argues against an RNA-mediated interaction between eIF4A and eIF4B. eIF4B_△NTD△RRM stimulates the ATPase and RNA unwinding activities of eIF4A and promotes the eIF4A conformational change to the closed state, yet it fails to stimulate recruitment of the PIC to mRNA.[16] The NTD is thus important for *in vivo* functions of eIF4B in translation initiation, but is dispensable for the stimulation of eIF4A ATPase and RNA unwinding activities *in vitro*.

The r1-7 region in isolation bound to eIF4A in the absence of eIF4G, but with severely reduced affinity. However, r1-7 on its own only moderately stimulates eIF4A activities, suggesting that communication of the r1-7 region with the NTD, CTD or RRM is required for full stimulation of eIF4A by eIF4B, for the recruitment of the PIC to the mRNA and for initiation of translation.

Materials and methods

Cloning, protein production and purification

The DNA coding sequences for *Saccharomyces cerevisiae* eIF4B were PCR-amplified from yeast Lambda genomic library S288c (Agilent Technologies) using oligonucleotide primers PB-001

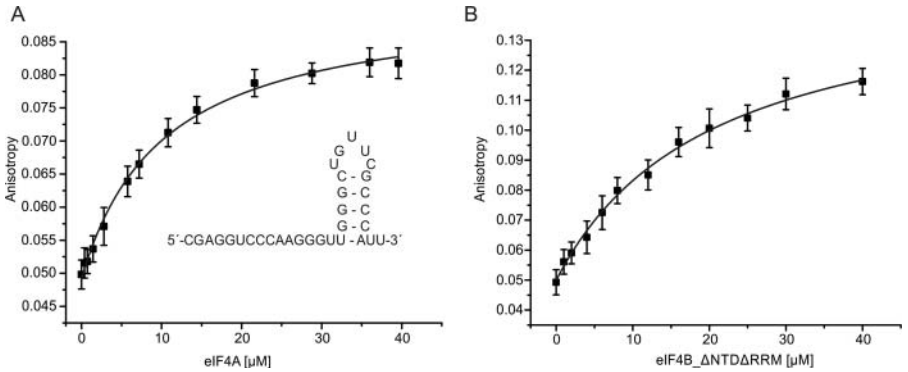

Figure 8. Binding of eIF4A and eIF4B_ΔNTDΔRRM to the 32mer RNA. (A) Fluorescence anisotropy titration of 5′-fluorescein-labeled 32mer with eIF4A in the presence of 10 mM ADPNP. The K_d for the eIF4A/32mer complex is $K_d = 10.3 \pm 1.3$ μM. Inset: 32mer RNA sequence and its secondary structure predicted by mfold.[37] (B) Fluorescence anisotropy titration of 5′-fluorescein-labeled 32mer with eIF4B_△NTDΔRRM. The K_d is 13.4 ± 0.6 μM. Representative binding curves; error bars represent anisotropy fluctuations. The errors of the K_d values are standard errors from 2 independent experiments.

and PB-012 (*tif3_ΔNTD*), PB-003, PB-011 (*tif3_ΔCTD*), PB-006 and PB-012 (*tif3_ΔNTDΔRRM*) or PB-009 and PB-010 (*tif3_r1-7*). *tif3_ΔRRM* and *tif3_Δr1-7* were generated by overlap-extension PCR. In a first round, overlapping fragments were amplified using PB-004, PB-011 and PB-005, PB-012 (*tif3_ΔRRM*) or PB-007, PB-011 and PB-008, PB-012 (*tif3_Δr1-7*). The PCR products of the individual reactions were annealed, and PCR-amplified with primers PB-011 and PB-012. The PCR product was inserted into the multiple cloning site of pET28a using restriction enzymes BamHI and NdeI. Primers used for cloning are summarized in Table S1. An eIF4B variant with cysteines at positions 248 and 274 (eIF4B_248C/274C) was generated according to the Quickchange protocol (Stratagene) using primers PB-0013 and PB-0014. All constructs were confirmed by sequencing. All eIF4B variants were recombinantly produced with an N-terminal His-tag in *E. coli* Rosetta(DE3), and purified to >95% purity as previously described.[9] eIF4B has a low secondary structure content, yet all deletion variants are stably produced and elute as a defined peak from a size-exclusion column. Similar circular dichroism (CD) spectra indicate similar secondary structure (Fig. S6). eIF4A_186C/370C, N-terminally biotinylated eIF4A_186C/370C (eIF4A-bio) and eIF4G_572–952 (eIF4G) were purified as described.[9,13] Fluorescently labeled eIF4B shows similar stimulation of eIF4A ATPase activity as wild-type eIF4B (Fig. S7).

Supernatant depletion experiments

Interactions between eIF4A, eIF4G and eIF4B variants were tested in supernatant depletion assays performed after Pollard.[22] Briefly, 130 μM eIF4A-bio was immobilized on streptavidin beads (Streptavidin Sepharose High Performance, GE Healthcare) in 30 mM Hepes/KOH pH 7.4, 100 mM KOAc, 3 mM Mg $(OAc)_2$, 2 mM DTT by incubation for 30 min at room temperature. Beads were centrifuged for 30 s at 1000 g, washed 3 times with buffer and resuspended in fresh buffer. For binding reactions 0 to 33 μM of eIF4A-bio (total concentration immobilized on beads) were mixed with 30 μl of 0.5 μM eIF4B (or 0.25 μM Alexa488-labeled eIF4B) in 30 mM Hepes/KOH pH 7.4, 100 mM KOAc, 3 mM $Mg(OAc)_2$, 2 mM DTT in the presence or absence of 2 or 15 μM eIF4G, 5 μM 32mer RNA (5′-CGAGG UCCCA AGGGU UGGGC UGUUC GCCCA UU-3′) and 10 mM ADPNP (Sigma-Aldrich) for 30 min. Intracellular concentrations of eIF4A and eIF4B are 50–60 μM and ~15 μM, respectively. The eIF4G concentration is also in the micromolar range.[23] The concentrations of the translation initiation factors in the supernatant depetion assays are therefore in a physiologically relevant range. After centrifugation at 15000 g, 24 μl of the supernatant were analyzed by SDS-PAGE. Bands were visualized by Coomassie Blue staining or Alexa488 fluorescence. The fraction bound was determined by densitometry. Each experiment was conducted with streptavidin beads without eIF4A-bio as a negative control in parallel.

Steady-state ATPase activity

The steady-state ATPase activity of eIF4A in the absence and presence of eIF4G and eIF4B variants was determined in a coupled enzymatic assay as described.[36] Experiments were performed in quartz cuvettes (Hellma analytics, Germany) in an Ultrospec 2100 pro UV/VIS Spectrophotometer (Amersham Biosciences, Germany) as previously described.[9] To determine $K_{M,app,RNA}$ values, data were described with the Michaelis-Menten equation.

RNA unwinding

PAGE-purified RNA oligonucleotides were purchased from Purimex (Grebenstein, Germany). Duplex RNA (25 μM) for unwinding reactions was prepared by annealing of a 32mer RNA modified with cyanine 5 (Cy5) at its 5′-end (5′Cy5-CGAGG UCCCA AGGGU UGGGC UGUUC GCCCA UU-3′) and a complementary 9mer modified with a cyanine 3 (Cy3) at the 3′-end (5′-UUGGGACCU-Cy3–3′) in 25 mM Hepes/KOH, pH 7.4. The mixture was heated to 96°C for 2 min, slowly cooled to room temperature and incubated on ice for 15 min. The stability of the duplex region was determined by the nearest neighbor method using mfold (version 2.3)[37] to −84 kJ mol^{-1} at 25°C. For the calculation, a 9-nucleotide loop connecting the duplex strands was introduced. Experiments were performed in 30 mM Hepes/KOH, pH 7.4, 100 mM KOAc, 3 mM $Mg(OAc)_2$, 2 mM DTT at 25°C with 500 nM duplex RNA, a 10-fold molar excess of unlabeled 9mer RNA to trap

the released 9mer (5′-AGG UCC CAA-3′) and ensure single turnover conditions, and 5 μM of eIF4A in the presence or absence of 5 μM eIF4G and 5 μM of the eIF4B variants. Unwinding reactions were initiated by the addition of 3 mM ATP after a stable fluorescence signal was obtained. All measurements were conducted in a Jobin Yvon FluoroMax3 fluorimeter. Cy3 fluorescence was excited at 554 nm (1 nm bandwidth) and Cy5 fluorescence was detected at 666 nm (3 nm bandwidth) in 10 s intervals with an integration time of 0.1 s. All measurements were repeated at least 3 times and the obtained unwinding curves were described by single exponential functions to determine the rate constant of unwinding. Experiments using a DNA trap gave similar results (Fig. S3).

Fluorescent labeling of eIF4A and eIF4B

eIF4A_186C/370C was labeled with Alexa488-maleimide (A488, donor) and Alexa546-maleimide (A546, acceptor) as previously described.[9] eIF4B_248C/274C was labeled with A488-maleimide. Labeling efficiencies were determined from absorbance spectra as described.[8,28] A488-labeled eIF4B retains the capability to stimulate RNA unwinding by eIF4A (Fig. S7).[8]

Single molecule FRET experiments

smFRET experiments were performed on a Microtime 200 confocal fluorescence microscope (PicoQuant GmbH, Germany) as previously described.[9] All measurements were performed with 100 pM labeled eIF4A (donor concentration), 10 μM of the indicated proteins (eIF4G and eIF4B variants), 3 mM ATP and 1 mM poly(U)-RNA in 50 mM Tris/HCl, pH 7.5, 80 mM KCl, 2.5 mM $MgCl_2$, 1 mM DTT and 1% glycerol at 25°C. Only fluorescence bursts over a threshold of 100 photons were considered for data analysis. Measured intensities were corrected for donor cross-talk into the acceptor channel, acceptor cross-talk into the donor channel, different quantum yields and detection efficiencies of donor and acceptor fluorescence, and direct excitation of the acceptor as previously described.[38] FRET histograms were created from fluorescent events taken from at least three different measurements performed on different days. To quantify the different eIF4A conformational states, FRET histograms were described with Gaussian distributions.

Fluorescence anisotropy titrations

Dissociation constants (K_d) for complex formation of eIF4A or eIF4B_ΔNTDΔRRM with RNA were determined by following the increase in fluorescence anisotropy of 50 nM 32mer, 5′-modified with 6-FAM (fluorescein), at 25°C in 30 mM Hepes/KOH, pH 7.4, 100 mM KOAc, 3 mM $Mg(OAc)_2$, 2 mM DTT. Binding experiments with eIF4A were performed in the presence of 10 mM ADPNP. Fluorescence was excited at 495 nm (2 nm bandwidth) and detected at 520 nm (5 nm bandwidth). K_d values were determined by fitting a 1:1 binding model to the anisotropy data by non-linear regression, taking into account the change in quantum yield of the dye upon complex formation, as previously described.[39]

CD spectroscopy

Far-UV CD spectra of eIF4B variants (0.25 mg ml^{-1}) in 10 mM HEPES/KOH pH 7.4, 100 mM NaCl were recorded from 200 to 260 nm at 25°C using a Jasco J-815 circular dichroism spectrometer. The scanning speed was 50 nm min^{-1}, the integration time was 0.5 s, and the path length 0.1 cm. Spectra were accumulated 10-fold and corrected for buffer contributions.

Disclosure of potential conflicts of interest

No potential conflicts of interest were disclosed.

Acknowledgments

We thank Jonathan Block and Christian Krause for performing preliminary experiments, Pavel Lulchev for help with circular dichroism measurements, and Daniela Schlingmeier for excellent technical assistance.

Funding

This work was funded by the Deutsche Forschungsgemeinschaft (KL1153/7–1).

References

1. Grifo JA, Tahara SM, Morgan MA, Shatkin AJ, Merrick WC. New initiation factor activity required for globin mRNA translation. J Biol Chem 1983; 258:5804-10; PMID:6853548
2. Sonenberg N, Morgan MA, Merrick WC, Shatkin AJ. A polypeptide in eukaryotic initiation factors that crosslinks specifically to the 5′-terminal cap in mRNA. Proc Natl Acad Sci U S A 1978; 75:4843-7; PMID:217002; http://dx.doi.org/10.1073/pnas.75.10.4843
3. Altmann M, Handschin C, Trachsel H. mRNA cap-binding protein: cloning of the gene encoding protein synthesis initiation factor eIF-4E from *Saccharomyces cerevisiae*. Mol Cell Biol 1987; 7:998-1003; PMID:3550438; http://dx.doi.org/10.1128/MCB.7.3.998
4. Goyer C, Altmann M, Lee HS, Blanc A, Deshmukh M, Woolford JL, Jr, Trachsel H, Sonenberg N. TIF4631 and TIF4632: two yeast genes encoding the high-molecular-weight subunits of the cap-binding protein complex (eukaryotic initiation factor 4F) contain an RNA recognition motif-like sequence and carry out an essential function. Mol Cell Biol 1993; 13:4860-74; PMID:8336723; http://dx.doi.org/10.1128/MCB.13.8.4860
5. Linder P, Slonimski PP. An essential yeast protein, encoded by duplicated genes TIF1 and TIF2 and homologous to the mammalian translation initiation factor eIF-4A, can suppress a mitochondrial missense mutation. Proc Natl Acad Sci U S A 1989; 86:2286-90; PMID:2648398; http://dx.doi.org/10.1073/pnas.86.7.2286
6. Svitkin YV, Pause A, Haghighat A, Pyronnet S, Witherell G, Belsham GJ, Sonenberg N. The requirement for eukaryotic initiation factor 4A (eIF4A) in translation is in direct proportion to the degree of mRNA 5′ secondary structure. RNA 2001; 7:382-94; PMID:11333019; http://dx.doi.org/10.1017/S135583820100108X
7. Jankowsky E, Gross CH, Shuman S, Pyle AM. Active disruption of an RNA-protein interaction by a DExH/D RNA helicase. Science 2001; 291:121-5; PMID:11141562; http://dx.doi.org/10.1126/science.291.5501.121
8. Hilbert M, Kebbel F, Gubaev A, Klostermeier D. eIF4G stimulates the activity of the DEAD box protein eIF4A by a conformational guidance mechanism. Nucleic Acids Res 2011; 39:2260-70; PMID:21062831; http://dx.doi.org/10.1093/nar/gkq1127
9. Andreou AZ, Klostermeier D. eIF4B and eIF4G jointly stimulate eIF4A ATPase and unwinding activities by modulation of the eIF4A conformational cycle. J Mol Biol 2014; 426:51-61; PMID:24080224; http://dx.doi.org/10.1016/j.jmb.2013.09.027

10. Sengoku T, Nureki O, Nakamura A, Kobayashi S, Yokoyama S. Structural Basis for RNA Unwinding by the DEAD-Box Protein Drosophila Vasa. Cell 2006; 125:287-300; PMID:16630817; http://dx.doi.org/10.1016/j.cell.2006.01.054
11. Rogers GW, Jr, Richter NJ, Lima WF, Merrick WC. Modulation of the helicase activity of eIF4A by eIF4B, eIF4H, and eIF4F. J Biol Chem 2001; 276:30914-22; PMID:11418588; http://dx.doi.org/10.1074/jbc.M100157200
12. Rogers GW, Jr, Richter NJ, Merrick WC. Biochemical and kinetic characterization of the RNA helicase activity of eukaryotic initiation factor 4A. J Biol Chem 1999; 274:12236-44; PMID:10212190; http://dx.doi.org/10.1074/jbc.274.18.12236
13. Harms U, Andreou AZ, Gubaev A, Klostermeier D. eIF4B, eIF4G and RNA regulate eIF4A activity in translation initiation by modulating the eIF4A conformational cycle. Nucleic Acids Res 2014; 42:7911-22; PMID:24848014; http://dx.doi.org/10.1093/nar/gku440
14. Schutz P, Bumann M, Oberholzer AE, Bieniossek C, Trachsel H, Altmann M, Baumann U. Crystal structure of the yeast eIF4A-eIF4G complex: An RNA-helicase controlled by protein-protein interactions. Proc Natl Acad Sci U S A 2008; 105:9564-9; PMID:18606994; http://dx.doi.org/10.1073/pnas.0800418105
15. Montpetit B, Thomsen ND, Helmke KJ, Seeliger MA, Berger JM, Weis K. A conserved mechanism of DEAD-box ATPase activation by nucleoporins and InsP6 in mRNA export. Nature 2011; 472:238-42; PMID:21441902; http://dx.doi.org/10.1038/nature09862
16. Walker SE, Zhou F, Mitchell SF, Larson VS, Valasek L, Hinnebusch AG, Lorsch JR. Yeast eIF4B binds to the head of the 40S ribosomal subunit and promotes mRNA recruitment through its N-terminal and internal repeat domains. RNA 2013; 19:191-207; PMID:23236192; http://dx.doi.org/10.1261/rna.035881.112
17. Niederberger N, Trachsel H, Altmann M. The RNA recognition motif of yeast translation initiation factor Tif3/eIF4B is required but not sufficient for RNA strand-exchange and translational activity. RNA 1998; 4:1259-67; PMID:9769100; http://dx.doi.org/10.1017/S1355838298980487
18. Rozovsky N, Butterworth AC, Moore MJ. Interactions between eIF4AI and its accessory factors eIF4B and eIF4H. RNA 2008; 14:2136-48; PMID:18719248; http://dx.doi.org/10.1261/rna.1049608
19. Nielsen KH, Behrens MA, He Y, Oliveira CL, Sottrup Jensen L, Hoffmann SV, Pedersen JS, Andersen GR. Synergistic activation of eIF4A by eIF4B and eIF4G. Nucleic Acids Res 2011; 15:67-75; PMID:21113024; http://dx.doi.org/10.1093/nar/gkg1206
20. Coppolecchia R, Buser P, Stotz A, Linder P. A new yeast translation initiation factor suppresses a mutation in the eIF-4A RNA helicase. EMBO J 1993; 12:4005-11; PMID:8404866
21. Park EH, Walker SE, Zhou F, Lee JM, Rajagopal V, Lorsch JR, Hinnebusch AG. Yeast Eukaryotic Initiation Factor (eIF) 4B enhances complex assembly between eIF4A and eIF4G in Vivo. J Biol Chem 2013; 288:2340-54; PMID:23184954; http://dx.doi.org/10.1074/jbc.M112.398537
22. Pollard TD. A guide to simple and informative binding assays. Mol Biol Cell 2010; 21:4061-7; PMID:21115850; http://dx.doi.org/10.1091/mbc.E10-08-0683
23. von der Haar T, McCarthy JE. Intracellular translation initiation factor levels in *Saccharomyces cerevisiae* and their role in cap-complex function. Mol Microbiol 2002; 46:531-44; PMID:12406227; http://dx.doi.org/10.1046/j.1365-2958.2002.03172.x
24. Rajagopal V, Park EH, Hinnebusch AG, Lorsch JR. Specific domains in yeast eIF4G strongly bias the RNA unwinding activity of the eIF4F complex towards duplexes with 5′-overhangs. J Biol Chem 2012; 287:20301-12; PMID:22467875; http://dx.doi.org/10.1074/jbc.M112.347278
25. Korneeva NL, First EA, Benoit CA, Rhoads RE. Interaction between the NH2-terminal domain of eIF4A and the central domain of eIF4G modulates RNA-stimulated ATPase activity. J Biol Chem 2005; 280:1872-81; PMID:15528191; http://dx.doi.org/10.1074/jbc.M406168200
26. Rozen F, Edery I, Meerovitch K, Dever TE, Merrick WC, Sonenberg N. Bidirectional RNA helicase activity of eucaryotic translation initiation factors 4A and 4F. Mol Cell Biol 1990; 10:1134-44; PMID:2304461; http://dx.doi.org/10.1128/MCB.10.3.1134
27. Steimer L, Wurm JP, Linden MH, Rudolph MG, Wohnert J, Klostermeier D. Recognition of two distinct elements in the RNA substrate by the RNA binding domain of the *T. thermophilus* DEAD box helicase Hera. Nucleic Acids Res 2013; 41:6259-72; PMID:23625962; http://dx.doi.org/10.1093/nar/gkt323
28. Theissen B, Karow AR, Kohler J, Gubaev A, Klostermeier D. Cooperative binding of ATP and RNA induces a closed conformation in a DEAD box RNA helicase. Proc Natl Acad Sci U S A 2008; 105:548-53; PMID:18184816; http://dx.doi.org/10.1073/pnas.0705488105
29. Ozes AR, Feoktistova K, Avanzino BC, Fraser CS. Duplex Unwinding and ATPase activities of the DEAD-Box Helicase eIF4A are coupled by eIF4G and eIF4B. J Mol Biol 2011; 412:674-87; PMID:21840318; http://dx.doi.org/10.1016/j.jmb.2011.08.004
30. Metz AM, Wong KC, Malmstrom SA, Browning KS. Eukaryotic initiation factor 4B from wheat and *Arabidopsis thaliana* is a member of a multigene family. Biochem Biophys Res Commun 1999; 266:314-21; PMID:10600500; http://dx.doi.org/10.1006/bbrc.1999.1814
31. Blum S, Schmid SR, Pause A, Buser P, Linder P, Sonenberg N, Trachsel H. ATP hydrolysis by initiation factor 4A is required for translation initiation in *Saccharomyces cerevisiae*. Proc Natl Acad Sci U S A 1992; 89:7664-8; PMID:1502180; http://dx.doi.org/10.1073/pnas.89.16.7664
32. Altmann M, Muller PP, Wittmer B, Ruchti F, Lanker S, Trachsel HA. *Saccharomyces cerevisiae* homologue of mammalian translation initiation factor 4B contributes to RNA helicase activity. EMBO J 1993; 12:3997-4003; PMID:8404865
33. Cheng S, Gallie DR. Wheat eukaryotic initiation factor 4B organizes assembly of RNA and eIFiso4G, eIF4A, and PABP. J Biol Chem 2006; 281:24351-64; PMID:16803875; http://dx.doi.org/10.1074/jbc.M605404200
34. Garcia-Garcia C, Frieda KL, Feoktistova K, Fraser CS, Block SM. Factor-dependent processivity in human eIF4A DEAD-box helicase. Science 2015; 348:1486-8; PMID:26113725; http://dx.doi.org/10.1126/science.aaa5089
35. Zhou F, Walker SE, Mitchell SF, Lorsch JR, Hinnebusch AG. Identification and characterization of functionally critical, conserved motifs in the internal repeats and N-terminal domain of yeast translation initiation factor 4B (yeIF4B). J Biol Chem 2014; 289:1704-22; PMID:24285537; http://dx.doi.org/10.1074/jbc.M113.529370
36. Adam H. Adenosin-5′diphosphat und Adenosin-5′monophosphat. Methoden der enzymatischen Analyse: Bergmeyer, H.U.(Hrsg.), Verlag Chemie, Weinheim 1962:573-7
37. Zuker M. Mfold web server for nucleic acid folding and hybridization prediction. Nucleic Acids Res 2003; 31:3406-15; PMID:12824337; http://dx.doi.org/10.1093/nar/gkg595
38. Andreou AZ, Klostermeier D. Conformational Changes of DEAD-Box helicases monitored by single molecule fluorescence resonance energy transfer. Methods Enzymol 2012; 511:75-109; PMID:22713316; http://dx.doi.org/10.1016/B978-0-12-396546-2.00004-8
39. Samatanga B, Klostermeier D. DEAD-box RNA helicase domains exhibit a continuum between complete functional independence and high thermodynamic coupling in nucleotide and RNA duplex recognition. Nucleic Acids Res 2014; 42:10644-54; PMID:25123660; http://dx.doi.org/10.1093/nar/gku747